Science Journal of Clinical Medicine
2026, Vol. 15, No. 1, pp. 1–10
https://doi.org/10.11648/j.sjcm.20261501.11

Research Article

Indocyanine Green Fluorescence Imaging-guided Hepatectomy for Hepatocellular Carcinoma Following Neoadjuvant Therapy

Man Luo[1, †], Yue Liu[1, †], Yaowei Hu[2], Hongguang Wang[1, *]

[1]Department of Hepatobiliary Surgery, National Cancer Center/National Clinical Research Center for Cancer/Cancer Hospital/Chinese Academy of Medical Sciences and Peking Union Medical College, Beijing, China

[2]Department of Hepatobiliary Surgery, Cancer Hospital Langfang Campus /Chinese Academy of Medical Sciences, Hebei, China

Abstract

Background: Neoadjuvant therapy has improved the resectability of locally advanced hepatocellular carcinoma (HCC), but treatment-induced tumor necrosis and fibrosis often obscure tumor boundaries, making margin control challenging during non-anatomical hepatectomy (NAH). This study evaluated the efficacy of indocyanine green (ICG) fluorescence imaging for tumor delineation and resection margin control in this patient population. Methods: This retrospective observational study included 110 patients with HCC who received neoadjuvant therapy and subsequently underwent NAH between January 2018 and January 2024. After exclusions, 88 eligible patients were divided into ICG-guided (n=40) and conventional surgery (n=48) groups, with 38 matched pairs (38 vs. 38) after 1: 1 propensity score matching (PSM). Primary outcomes included adequate/positive resection margin rates and boundary identification accuracy; secondary outcomes were perioperative and oncological outcomes. Results: The ICG group demonstrated a significantly higher adequate margin rate (92.1% vs. 73.7%, p = 0.034) and improved tumor boundary identification accuracy (89.5% vs. 63.2%, p = 0.012). The positive margin rate was lower in the ICG group (2.6% vs. 18.4%, p = 0.058). Length of hospital stay was significantly shorter (7.1 ± 2.0 vs. 9.4 ± 2.7 days, p = 0.001), while operative time, blood loss, and postoperative complication rates were comparable. No significant differences in recurrence-free survival (RFS) or overall survival (OS) were observed. Conclusions: ICG fluorescence imaging enhances tumor boundary visualization and may improve resection margin quality in NAH following neoadjuvant therapy for HCC, representing a valuable intraoperative navigation tool.

Keywords

Hepatocellular Carcinoma, Neoadjuvant Therapy, Indocyanine Green, Fluorescence Imaging, R0 Resection, Hepatectomy, Surgical Margin

*Correspondence: Hongguang Wang (wanghongguangNCC@126.com)

† Man Luo and Yue Liu are co-first authors.

Received: 29 March 2026; **Accepted:** 16 April 2026; **Published:** 28 April 2026

1. Introduction

Hepatocellular carcinoma (HCC) remains one of the leading causes of cancer-related mortality worldwide, with surgical resection standing as the primary curative treatment for eligible patients [1]. In recent years, neoadjuvant therapy, including targeted therapy, immunotherapy, and transarterial chemoembolization (TACE), has increasingly emerged as a transformative strategy for locally advanced HCC [2, 3]. By downstaging tumors, reducing micrometastatic burden, and improving resectability, this approach has expanded curative opportunities for patients who were previously deemed inoperable [4-6]. However, even with favorable tumor response, a substantial subset of these patients are not candidates for anatomical or territorial hepatectomy due to severe liver cirrhosis, insufficient future liver remnant, deep tumor location, or unfavorable tumor distribution. For this high-risk group, non-anatomical hepatectomy (NAH) represents the only feasible curative approach, balancing tumor clearance with the preservation of functional liver parenchyma [7, 8].

The success of NAH hinges on accurate identification of viable tumor boundaries and achievement of adequate resection margins—two factors directly linked to local recurrence and long-term survival [9]. Unfortunately, neoadjuvant therapy frequently induces treatment-related pathological changes, including tumor necrosis, fibrosis, and inflammatory infiltration, which obscure the distinction between viable tumor tissue and surrounding normal liver parenchyma [10, 11]. Conventional visualization methods, including visual inspection, palpation, and intraoperative ultrasound, often fail to reliably delineate biological tumor boundaries in this setting, leading to suboptimal resection margins, increased positive margin rates, and compromised oncological outcomes. This unmet clinical need highlights the urgent demand for a real-time, precise navigation tool to enhance surgical decision-making in post-neoadjuvant HCC patients undergoing non-anatomical resection.

Indocyanine green (ICG) fluorescence imaging has emerged as a promising intraoperative navigation technique in hepatobiliary surgery. Leveraging impaired biliary excretion in malignant hepatocytes, ICG is selectively retained in viable tumor tissue, enabling real-time visualization of biological tumor boundaries rather than relying solely on morphological features [12, 13]. This unique advantage has been validated in various complex liver surgical scenarios, including difficult laparoscopic hepatectomy, where it has been shown to shorten operative time and reduce postoperative complications [14]. ICG fluorescence imaging also facilitates precise preoperative and intraoperative localization of liver lesions, real-time visualization of hepatic anatomy, and accurate definition of resection margins—key requirements for preserving liver parenchyma and improving surgical safety [15]. However, studies specifically evaluating the efficacy of ICG fluorescence imaging in patients who receive neoadjuvant therapy and require NAH remain limited. Existing evidence primarily focuses on unselected HCC populations, and data regarding its utility in overcoming neoadjuvant therapy-induced boundary obscurity are scarce.

To address this research gap, the present retrospective study aimed to investigate the value of ICG fluorescence imaging-guided tumor delineation and resection margin control in HCC patients following neoadjuvant therapy who were ineligible for anatomical resection [16]. We hypothesized that ICG-guided navigation would improve the accuracy of viable tumor identification, optimize resection margin quality, and enhance both perioperative and oncological outcomes compared with conventional surgical methods. The findings of this study seek to provide clinical evidence for refining surgical strategies in this challenging patient cohort.

2. Materials and Methods

2.1. Study Design and Patients

This was a retrospective observational study approved by the Ethics Committee of National Cancer Center (NCC2021C-239), and the requirement for informed consent was waived due to the retrospective nature of the study. Consecutive patients diagnosed with HCC who received neoadjuvant therapy and subsequently underwent NAH at our institution between January 2018 and January 2024 were enrolled.

The inclusion criteria were: (1) Pathologically confirmed HCC; (2) Received at least one cycle of neoadjuvant therapy (targeted therapy, immunotherapy, TACE, or combination therapy); (3) Evaluated as ineligible for anatomical hepatectomy (AH) by a multidisciplinary (MDT) team due to severe liver cirrhosis, insufficient future liver remnant (FLR) (<30% for non-cirrhotic liver, <50% for cirrhotic liver), deep tumor location (involving central hepatic veins or portal vein branches), or multifocal lesions not suitable for segmental resection; (4) Underwent NAH; (5) Complete clinical, surgical, and follow-up data available.

The exclusion criteria were: (1) Contraindications to ICG (e.g., hypersensitivity to ICG or iodine); (2) Diffuse HCC or tumor involvement of more than 50% of the liver parenchyma; (3) Extrahepatic metastasis or vascular invasion (portal vein tumor thrombus, hepatic vein tumor thrombus); (4) Concurrent other malignant tumors; (5) Severe cardiopulmonary, renal, or hematological diseases that cannot tolerate surgery.

Eligible patients were divided into an ICG-guided surgery group and a conventional surgery group according to the surgical navigation method used during the study period. Propensity score matching (PSM) was performed using a logistic regression model to balance baseline characteristics between the two groups, with a ratio of 1: 1, including the following covariates: age, sex, Child–Pugh class, tumor size, tumor number, AFP level, and neoadjuvant therapy regimen. Nearest-neighbor matching with a caliper width of 0.2 was applied.

2.2. Neoadjuvant Therapy

Neoadjuvant therapy regimens were determined by the MDT team based on the patient's liver function, tumor characteristics, and general condition, including: (1) Targeted therapy (e.g., sorafenib, lenvatinib); (2) Immune checkpoint inhibitors (e.g., nivolumab, pembrolizumab); (3) Transarterial chemoembolization (TACE); (4) Combination therapy (e.g., targeted therapy plus immunotherapy, TACE plus targeted therapy). All patients completed at least one cycle of neoadjuvant therapy, and the treatment was discontinued 2–4 weeks before surgery to reduce the risk of intraoperative bleeding and postoperative complications. Tumor response was evaluated using the Response Evaluation Criteria in Solid Tumors (RECIST) version 1.1 based on contrast-enhanced computed tomography (CT) or magnetic resonance imaging (MRI) performed 1–2 weeks before surgery, which was classified as complete response (CR), partial response (PR), stable disease (SD), or progressive disease (PD).

2.3. Surgical Procedures

In the ICG-guided group, ICG (Indocyanine Green Injection, Ruidu, China) was injected intravenously at a dose of 0.5 mg/kg 24–48 h before surgery. During NAH, a dedicated surgical fluorescence imaging system was used to identify viable tumor regions in real time. The resection plane was determined as 5–10 mm outside the fluorescent boundary of the viable tumor to ensure adequate resection margins. Intraoperative frozen section examination was performed for suspected positive margins to confirm tumor clearance.

In the conventional group, surgery was performed using visual inspection, palpation, and intraoperative ultrasound without fluorescence navigation. The resection plane was determined based on the intraoperative ultrasound findings and the surgeon's experience, with the goal of achieving a 5–10 mm resection margin. Intraoperative frozen section examination was also performed for suspected positive margins.

Both groups received standard perioperative management and surgical techniques.

2.4. Outcome Measures

2.4.1. Primary Outcomes

Rate of adequate resection margins (defined as resection margin ≥5 mm on postoperative pathological examination, without residual viable tumor cells).

Positive resection margin rate (defined as residual viable tumor cells at the resection margin on postoperative pathological examination).

Accuracy of viable tumor boundary identification (defined as the concordance between intraoperative tumor boundary estimation and pathological tumor boundary measured in the resected specimen).

2.4.2. Secondary Outcomes

Operative time (from skin incision to skin closure).

Intraoperative blood loss (measured by the volume of blood collected in the suction device and the weight of gauze used).

Postoperative complications (classified according to the Clavien-Dindo classification system, grade ≥3 complications were considered major complications).

Length of hospital stay (from the day of surgery to the day of discharge).

2.5. Statistical Analysis

All data were collected from the hospital electronic medical record system and follow-up records. Continuous variables were expressed as mean ± standard deviation (for normally distributed data) or median (interquartile range, IQR) (for non-normally distributed data) and compared using the Student's t-test or Mann–Whitney U test, respectively. Categorical variables were presented as numbers (percentages) and analyzed using the chi-square test or Fisher's exact test, as appropriate. Propensity score matching (PSM) was performed using the nearest neighbor method with a caliper of 0.2 to balance baseline characteristics between the two groups. Kaplan–Meier survival curves were constructed to evaluate recurrence-free survival (RFS) and overall survival (OS), and differences between groups were compared using the log-rank test. Cox proportional hazards regression models were used to estimate hazard ratios (HRs) and 95% confidence intervals (CIs) for recurrence-free survival and overall survival. Because the incidence of positive resection margins was extremely low after propensity score matching, Fisher's exact test was used to compare the incidence of positive margins between groups rather than performing logistic regression analysis. A p-value < 0.05 was considered statistically significant. All statistical analyses were performed using SPSS 26.0 software. Variables with $p < 0.10$ in univariate analysis were included in the multivariate models.

3. Results

3.1. Patient Enrollment and Baseline Characteristics

A total of 110 patients with hepatocellular carcinoma (HCC) who received neoadjuvant therapy and subsequently underwent non-anatomical hepatectomy were initially screened. After applying the exclusion criteria, 22 patients were excluded, leaving 88 eligible patients for further analysis. Among them, 40 patients underwent ICG fluorescence-guided surgery, while 48 patients underwent conventional surgery.

To minimize potential selection bias, propensity score matching (PSM) was performed using a 1: 1 nearest-neighbor method, resulting in 38 matched pairs (38 vs. 38) included in the final analysis (Figure 1).

After PSM, baseline characteristics between the two groups were well balanced. All standardized mean differences after matching were below the commonly accepted threshold of 0.1, indicating adequate balance between groups.

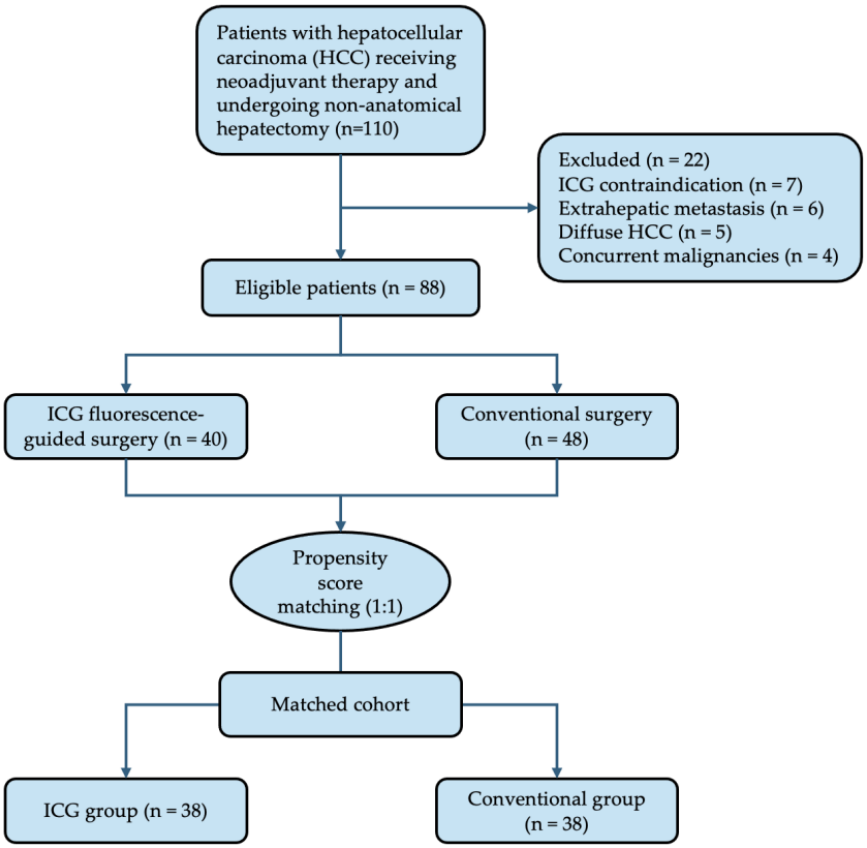

Figure 1. *Patient selection flowchart. A total of 110 patients were screened, and 88 eligible patients were included. After 1: 1 propensity score matching, 38 matched pairs were analyzed.*

After PSM, baseline characteristics between the two groups were well balanced (Table 1). The mean age of patients in the ICG group and conventional group was 58.2 ± 7.9 years and 57.7 ± 8.3 years, respectively. The majority of patients were male (76.3% in the ICG group vs. 71.1% in the conventional group). In terms of liver function, most patients were classified as Child-Pugh class A (84.2% vs. 78.9%). The median tumor size was 4.1 cm (IQR: 3.0–5.4 cm) in the ICG group and 4.4 cm (IQR: 3.2–5.7 cm) in the conventional group. The most common neoadjuvant therapy regimen was combination therapy (targeted + immunotherapy) in both groups (42.1% vs. 39.5%), and the partial response (PR) rate to neoadjuvant therapy was comparable between the two groups (65.8% vs. 60.5%). No significant difference was observed in preoperative alpha-fetoprotein (AFP) levels (median: 125.3 ng/mL vs. 132.6 ng/mL, $p = 0.689$). No statistically significant differences were observed in baseline characteristics (all $p > 0.05$).

Table 1. *Baseline characteristics of patients before and after propensity score matching (PSM). Before PSM: 40 vs 48 eligible; After PSM: 38 vs 38 eligible.*

Characteristic	ICG group (n=38)	Conventional group (n=38)	p-value
Age, mean ± SD (years)	58.2 ± 7.9	57.7 ± 8.3	0.762
Gender, n (%)			0.598
Male	29 (76.3)	27 (71.1)	
Female	9 (23.7)	11 (28.9)	
Child-Pugh class, n (%)			0.526

Characteristic	ICG group (n=38)	Conventional group (n=38)	p-value
Class A	32 (84.2)	30 (78.9)	
Class B	6 (15.8)	8 (21.1)	
Tumor size, median (IQR) (cm)	4.1 (3.0–5.4)	4.4 (3.2–5.7)	0.498
Tumor number, n (%)			0.431
Single	35 (92.1)	33 (86.8)	
Multiple (2–3)	3 (7.9)	5 (13.2)	
AFP, median (IQR) (ng/mL)	125.3 (44.8–281.5)	132.6 (47.9–295.2)	0.689
Neoadjuvant therapy regimen, n (%)			0.793
Targeted therapy	9 (23.7)	10 (26.3)	
Immunotherapy	7 (18.4)	6 (15.8)	
TACE	6 (15.8)	7 (18.4)	
Combination therapy	16 (42.1)	15 (39.5)	
Tumor response, n (%)			0.587
Complete response (CR)	2 (5.3)	1 (2.6)	
Partial response (PR)	25 (65.8)	23 (60.5)	
Stable disease (SD)	11 (28.9)	14 (36.8)	
Progressive disease (PD)	0 (0.0)	0 (0.0)	

3.2. Primary Outcomes: Tumor Delineation and Resection Margin Control

The primary outcomes focused on resection margin quality and tumor boundary identification (Table 2).

The adequate resection margin rate (≥5 mm) was significantly higher in the ICG group (92.1% vs. 73.7%, p = 0.034).

The positive margin rate showed a trend toward reduction in the ICG group (2.6% vs. 18.4%), although the difference did not reach statistical significance (p = 0.058).

Furthermore, the accuracy of tumor boundary identification was significantly improved in the ICG group (89.5% vs. 63.2%, p = 0.012).

Table 2. *Comparison of primary outcomes between the two groups after PSM.*

Primary Outcome	ICG group (n=38)	Conventional group (n=38)	p-value
Adequate resection margins ≥5mm, n (%)	35 (92.1)	28 (73.7)	0.034
Positive resection margins, n (%)	1 (2.6)	7 (18.4)	0.058
Boundary accuracy, n (%)	34 (89.5)	24 (63.2)	0.012

3.3. Perioperative Outcomes

Perioperative outcomes are summarized in Table 3. There were no significant differences in operative time (155.6 ±32.5 vs. 161.2 ±34.9 min, p = 0.415) or intraoperative blood loss (282.4 ±123.5 vs. 325.8 ±139.7 mL, p = 0.178). However, the length of hospital stay was significantly shorter in the ICG group (7.1 ±2.0 days vs. 9.4 ±2.7 days, p = 0.001).

Table 3. Comparison of secondary outcomes between the two groups after PSM.

Secondary Outcome	ICG group (n=38)	Conventional group (n=38)	p-value
Operative time, mean ± SD (min)	155.6 ± 32.5	161.2 ± 34.9	0.415
Intraoperative blood loss, mean ± SD (mL)	282.4 ± 123.5	325.8 ± 139.7	0.178
Length of hospital stay, mean ± SD (days)	7.1 ± 2.0	9.4 ± 2.7	0.001

3.4. Oncological Outcomes

The median follow-up time was 16.2 months (IQR: 12.5–20.3 months). Kaplan–Meier survival analysis was performed to evaluate the oncological outcomes between the ICG-guided hepatectomy group and the conventional hepatectomy group.

Recurrence-free survival (RFS): Kaplan–Meier analysis showed that patients undergoing ICG-guided hepatectomy had a numerically higher RFS probability compared with those undergoing conventional surgery (p = 0.181) (Figure 2).

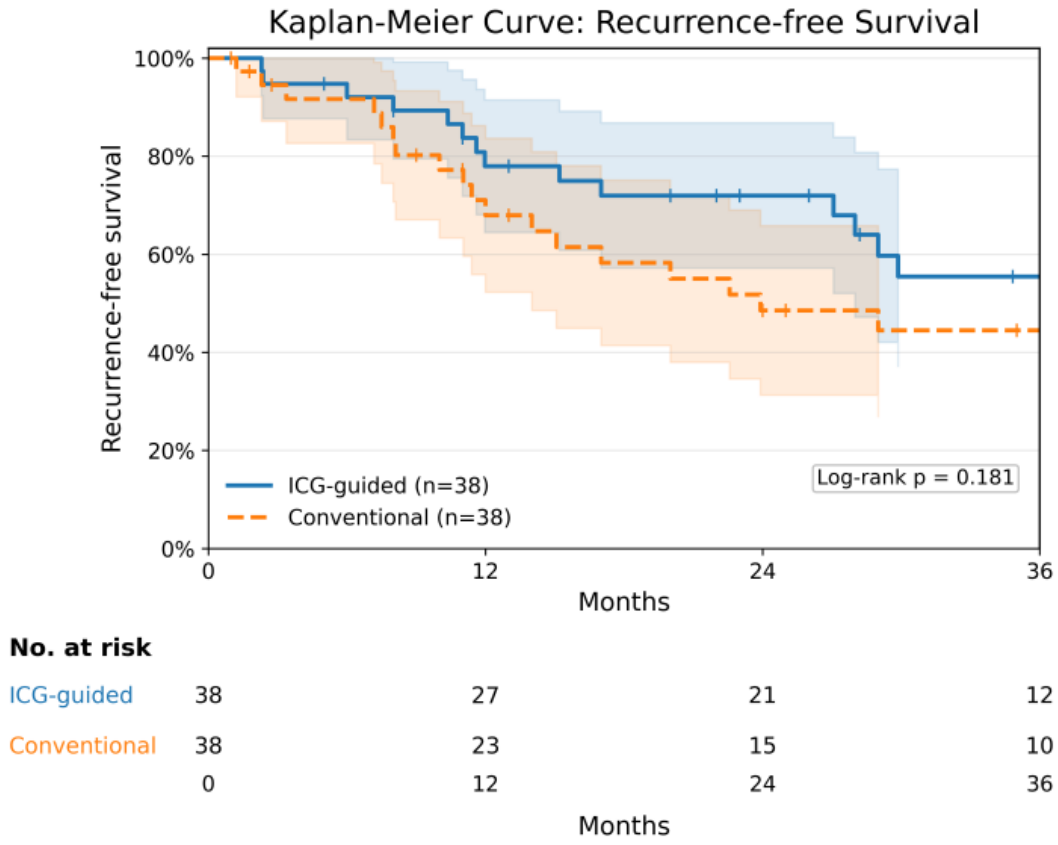

Figure 2. Kaplan–Meier curves of recurrence-free survival (RFS) in patients undergoing ICG-guided hepatectomy versus conventional surgery after propensity score matching. The ICG-guided group demonstrated a trend toward improved recurrence-free survival compared with the conventional group, although the difference did not reach statistical significance (p = 0.181). Follow-up time is presented in months.

Overall Survival (OS): For overall survival, Kaplan–Meier analysis demonstrated no significant difference between the two groups (p = 0.376) (Figure 3). Cox regression analysis showed that the risk of mortality was comparable between groups.

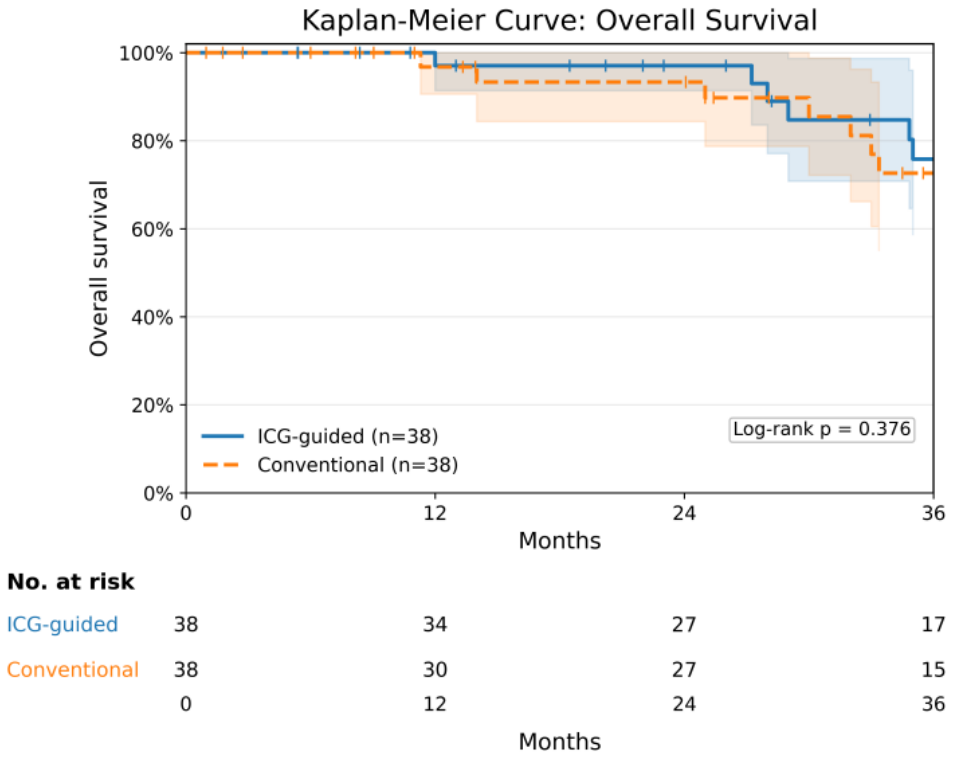

Figure 3. *Kaplan–Meier curves of overall survival (OS) in patients undergoing ICG-guided hepatectomy versus conventional surgery after propensity score matching. No significant difference in overall survival was observed between the two groups (p = 0.376). Follow-up time is presented in months.*

Overall, these findings suggest that ICG-guided hepatectomy may reduce the risk of early recurrence and show a trend toward improved recurrence-free survival, although no statistically significant survival advantage was observed during the current follow-up period.

3.5. Postoperative Complications

The overall incidence of postoperative complications was 21.1% in the ICG group and 26.3% in the conventional group, with no significant difference (p = 0.567) (Table 4). The most common complications were:

Bile leakage: 10.5% in the ICG group vs. 13.2% in the conventional group (p = 0.738).

Abdominal infection: 5.3% vs. 7.9% (p = 0.679).

Transient hepatic dysfunction: 5.3% in both groups (p = 1.000).

The incidence of major complications (Clavien-Dindo grade ≥3) was 5.3% in the ICG group (1 case of severe bile leakage requiring endoscopic stenting, 1 case of abdominal infection requiring percutaneous drainage) and 7.9% in the conventional group (2 cases of severe bile leakage, 1 case of gastrointestinal bleeding), with no significant difference (p = 0.679). All complications were resolved with conservative or interventional treatment, and no postoperative mortality occurred in either group.

Table 4. *Postoperative complications between the two groups after PSM.*

Complication Type	ICG group (n=38), n (%)	Conventional group (n=38), n (%)	p-value
Overall complications	8 (21.1)	10 (26.3)	0.567
Bile leakage	4 (10.5)	5 (13.2)	0.738
Abdominal infection	2 (5.3)	3 (7.9)	0.679
Transient hepatic dysfunction	2 (5.3)	2 (5.3)	1.000
Major complications (Grade ≥3)	2 (5.3)	3 (7.9)	0.679

3.6. Risk Factor Analysis

To identify factors associated with tumor recurrence, Cox proportional hazards regression analysis was performed for recurrence-free survival (RFS) after propensity score matching (Table 5). In the multivariable model, immunotherapy was identified as an independent protective factor for recurrence (HR = 0.39, 95% CI 0.18–0.84, p = 0.020). Tumor multiplicity and AFP level showed no significant association with recurrence. ICG-guided surgery demonstrated a protective trend but did not reach statistical significance (HR = 0.53, 95% CI 0.24–1.16, p = 0.119).

Table 5. *Cox proportional hazards regression analysis for recurrence-free survival.*

Variable	Univariable HR (95% CI)	p-value	Multivariable HR (95% CI)	p-value
AFP ≥ 400 ng/mL	1.73 (0.87–3.46)	0.118	1.69 (0.84–3.38)	0.142
ICG fluorescence guidance	0.56 (0.27–1.18)	0.129	0.53 (0.24–1.16)	0.119
Immunotherapy	0.41 (0.20–0.86)	0.019	0.39 (0.18–0.84)	0.020
Margin <5 mm	1.19 (0.44–3.20)	0.733	1.15 (0.43–3.07)	0.774
Multiple tumors	1.44 (0.74–2.79)	0.279	1.33 (0.68–2.61)	0.395

The incidence of positive resection margins was low after propensity score matching (1 vs. 7 cases). Fisher's exact test showed a trend toward a lower positive margin rate in the ICG-guided group, although the difference did not reach statistical significance (p = 0.058).

4. Discussion

This study evaluated the clinical value of ICG fluorescence imaging for tumor delineation and resection margin control during non-anatomical hepatectomy (NAH) in hepatocellular carcinoma (HCC) patients who received neoadjuvant therapy and were not suitable candidates for anatomical hepatectomy. After propensity score matching, ICG fluorescence guidance was associated with a higher rate of adequate resection margins and improved tumor boundary identification. A trend toward a lower positive margin rate was observed in the ICG-guided group, although it did not reach statistical significance. Additionally, ICG guidance was associated with shorter postoperative hospital stay and a trend toward improved recurrence-free survival, without increasing operative time, intraoperative blood loss, or postoperative complications. These findings suggest that fluorescence-guided surgery may enhance surgical precision and improve perioperative outcomes in this challenging clinical scenario.

Fluorescence-guided liver surgery has attracted increasing attention. Multiple studies have demonstrated that ICG fluorescence imaging can assist intraoperative tumor detection, lesion localization, and surgical margin assessment [17, 18]. However, evidence in post-neoadjuvant therapy patients remains limited. In this population, treatment-induced necrosis and fibrosis may obscure tumor boundaries, making conventional assessment methods, such as visual inspection, palpation, and intraoperative ultrasonography, insufficient to delineate viable tumor tissue accurately [19]. ICG fluorescence imaging provides biologically based visualization that facilitates more precise intraoperative tumor localization.

ICG is selectively retained in malignant hepatocytes due to impaired biliary excretion. This allows near-infrared fluorescence imaging to highlight tumor tissue and delineate boundaries in real time. This mechanism is particularly valuable after neoadjuvant therapy, where viable tumor tissue may coexist with necrotic or fibrotic areas. Previous studies have reported that ICG fluorescence imaging can detect over 90% of malignant liver lesions and reveal small satellite nodules not identified by conventional imaging modalities [20]. Such biological visualization may enhance intraoperative tumor identification and improve resection margin control.

Another key observation in this study is the improvement in resection margin quality with ICG guidance. Adequate surgical margins are a key determinant of oncological outcomes after HCC resection. While anatomical hepatectomy (AH) is often recommended to remove the entire portal venous territory potentially containing microscopic tumor spread, AH may not be feasible in patients with impaired liver function, insufficient future liver remnant, or tumors in anatomically complex regions [21]. In such cases, NAH is performed as a parenchyma-sparing alternative, but this may increase the risk of inadequate margins. Fluorescence-guided surgery allows real-time visualization of tumor tissue, enabling surgeons to define boundaries precisely and adjust the resection plane during parenchymal transection. The higher adequate margin rate observed in the ICG group supports this advantage.

This study specifically focused on HCC patients who received neoadjuvant therapy and required NAH, a population that has been largely underrepresented in previous literature

[22]. By addressing this subgroup, our findings highlight the potential value of fluorescence navigation in overcoming treatment-induced tissue changes that obscure tumor boundaries. The observed trends toward lower recurrence and improved surgical precision suggest that ICG guidance may enhance oncological radicality, although longer follow-up is needed to determine its impact on long-term survival.

Several limitations should be noted. First, this study was retrospective and conducted at a single center, which may introduce selection bias despite the use of propensity score matching. Second, the sample size was relatively small, which may limit statistical power. Third, follow-up duration was limited for evaluating long-term outcomes such as overall survival and disease-free survival. Variations in the timing and dosage of ICG administration may also influence fluorescence signal intensity and imaging quality. Standardization of ICG injection protocols could improve reproducibility and clinical utility. Future prospective multicenter studies with larger sample sizes and longer follow-up are warranted to validate these findings.

5. Conclusions

In conclusion, this study provides evidence supporting the use of ICG fluorescence imaging for tumor delineation and resection margin control during NAH in HCC patients following neoadjuvant therapy who are not candidates for anatomical resection. By improving intraoperative visualization and enabling more precise surgical resection without increasing perioperative risk, fluorescence-guided surgery represents a promising strategy to optimize surgical precision and oncological outcomes in this high-risk patient population.

Abbreviations

HCC	Hepatocellular Carcinoma
AH	Anatomical Hepatectomy
NAH	Non-Anatomical Hepatectomy
ICG	Indocyanine Green
FLR	Future Liver Remnant
OS	Overall Survival
RFS	Recurrence-Free Survival
PSM	Propensity Score Matching
TACE	Transarterial Chemoembolization
AFP	Alpha-Fetoprotein

Acknowledgments

The authors have reviewed and edited the output and take full responsibility for the content of this publication.

Author Contributions

Man Luo: Conceptualization, Formal Analysis, Methodology, Software, Writing – original draft

Yue Liu: Data curation, Investigation

Yaowei Hu: Data curation

Hongguang Wang: Funding acquisition, Supervision, Validation, Visualization

Funding

This research was funded by National Natural Science Foundation of China, grant number 82473496, 82272963.

Data Availability Statement

The data is available from the corresponding author upon reasonable request.

Conflicts of Interest

The authors declare no conflicts of interest.

References

[1] Arnold, M.; Abnet, C. C.; Neale, R. E.; Vignat, J.; Giovannucci, E. L.; McGlynn, K. A.; Bray, F. Global Burden of 5 Major Types of Gastrointestinal Cancer. *Gastroenterology* 2020, *159*, https://doi.org/10.1053/j.gastro.2020.02.068

[2] Ho, W. J.; Zhu, Q.; Durham, J.; Popovic, A.; Xavier, S.; Leatherman, J.; Mohan, A.; Mo, G.; Zhang, S.; Gross, N.; et al. Neoadjuvant Cabozantinib and Nivolumab Converts Locally Advanced HCC into Resectable Disease with Enhanced Antitumor Immunity. *Nat Cancer* 2021, *2*, 891-903, https://doi.org/10.1038/s43018-021-00234-4

[3] Qin, S.; Chen, M.; Cheng, A.-L.; Kaseb, A. O.; Kudo, M.; Lee, H. C.; Yopp, A. C.; Zhou, J.; Wang, L.; Wen, X.; et al. Atezolizumab plus bevacizumab versus active surveillance in patients with resected or ablated high-risk hepatocellular carcinoma (IMbrave050): a randomised, open-label, multicentre, phase 3 trial. *Lancet* 2023, *402*, 1835-1847, https://doi.org/10.1016/S0140-6736(23)01796-8

[4] Llovet, J. M.; Pinyol, R.; Yarchoan, M.; Singal, A. G.; Marron, T. U.; Schwartz, M.; Pikarsky, E.; Kudo, M.; Finn, R. S. Adjuvant and neoadjuvant immunotherapies in hepatocellular carcinoma. *Nat Rev Clin Oncol* 2024, *21*, 294-311, https://doi.org/10.1038/s41571-024-00868-0

[5] Savic, L. J.; Chen, E.; Nezami, N.; Murali, N.; Hamm, C. A.; Wang, C.; Lin, M.; Schlachter, T.; Hong, K.; Georgiades, C.; et al. Conventional vs. Drug-Eluting Beads Transarterial Chemoembolization for Unresectable Hepatocellular Carcinoma-A Propensity Score Weighted Comparison of Efficacy and Safety. *Cancers (Basel)* 2022, *14*, https://doi.org/10.3390/cancers14235847

[6] Kawaguchi, Y.; Hasegawa, K.; Kashiwabara, K.; Okamura, Y.; Kurosaki, M.; Kudo, M.; Shimada, M.; Yamanaka, N.; Inomata, M.; Yamashita, T.; et al. Surgery Versus Ablation for Hepatocellular Carcinoma: A Randomized Controlled Trial (SURF-RCT Trial) and a Nonrandomized Prospective Observational Trial (SURF-Cohort Trial). *J Clin Oncol* 2025, *43*, 2628-2638, https://doi.org/10.1200/JCO-24-02030

[7] Zeindler, J.; Hess, G. F.; von Heesen, M.; Aegerter, N.; Reber, C.; Schmitt, A. M.; Muenst, S.; Bolli, M.; Soysal, S. D.; Kollmar, O. Anatomic versus non-anatomic liver resection for hepatocellular carcinoma-A European multicentre cohort study in cirrhotic and non-cirrhotic patients. *Cancer Med* 2024, *13*, e6981, https://doi.org/10.1002/cam4.6981

[8] Liao, K.; Yang, K.; Cao, L.; Lu, Y.; Zheng, B.; Li, X.; Wang, X.; Li, J.; Chen, J.; Zheng, S. Laparoscopic Anatomical Versus Non-anatomical hepatectomy in the Treatment of Hepatocellular Carcinoma: A randomised controlled trial. *Int J Surg* 2022, *102*, 106652, https://doi.org/10.1016/j.ijsu.2022.106652

[9] Tsilimigras, D. I.; Sahara, K.; Moris, D.; Hyer, J. M.; Paredes, A. Z.; Bagante, F.; Merath, K.; Farooq, A. S.; Ratti, F.; Marques, H. P.; et al. Effect of Surgical Margin Width on Patterns of Recurrence among Patients Undergoing R0 Hepatectomy for T1 Hepatocellular Carcinoma: An International Multi-Institutional Analysis. *J Gastrointest Surg* 2019, *24*, 1552-1560, https://doi.org/10.1007/s11605-019-04275-0

[10] Vogel, A.; Grant, R. C.; Meyer, T.; Sapisochin, G.; O'Kane, G. M.; Saborowski, A. Adjuvant and neoadjuvant therapies for hepatocellular carcinoma. *Hepatology* 2023, *82*, 777-793, https://doi.org/10.1097/HEP.0000000000000726

[11] Singal, A. G.; Yarchoan, M.; Yopp, A.; Sapisochin, G.; Pinato, D. J.; Pillai, A. Neoadjuvant and adjuvant systemic therapy in HCC: Current status and the future. *Hepatol Commun* 2024, *8*, https://doi.org/10.1097/HC9.0000000000000430

[12] Xiong, Y.; He, P.; Zhang, Y.; Chen, H.; Peng, Y.; He, P.; Tian, J.; Cheng, H.; Liu, G.; Li, J. Superstable homogeneous lipiodol-ICG formulation: initial feasibility and first-in-human clinical application for ruptured hepatocellular carcinoma. *Regen Biomater* 2022, *10*, rbac106, https://doi.org/10.1093/rb/rbac106

[13] Mao, T.; Xie, Q.; Zhao, X.; Jiang, K.; Yang, M.; Gao, F. Indocyanine green fluorescence imaging (ICG-FI) in difficult laparoscopic hepatectomy for hepatocellular carcinoma: a retrospective propensity score-matched analysis. *Surg Endosc* 2025, *39*, 3400-3411, https://doi.org/10.1007/s00464-025-11707-3

[14] Wakabayashi, T.; Cacciaguerra, A. B.; Abe, Y.; Bona, E. D.; Nicolini, D.; Mocchegiani, F.; Kabeshima, Y.; Vivarelli, M.; Wakabayashi, G.; Kitagawa, Y. Indocyanine Green Fluorescence Navigation in Liver Surgery: A Systematic Review on Dose and Timing of Administration. *Ann Surg* 2022, *275*, 1025-1034, https://doi.org/10.1097/SLA.0000000000005406

[15] Zhou, J.; Tan, Z.; Sun, B.; Leng, Y.; Liu, S. Application of indocyanine green fluorescence imaging in hepatobiliary surgery. *Int J Surg* 2024, *110*, 7948-7961, https://doi.org/10.1097/JS9.0000000000001802

[16] Gan, Y.-X.; Yang, Z.-L.; Pan, Y.-X.; Ou-Yang, L.-Y.; Tang, Y.-H.; Zhang, Y.-J.; Chen, M.-S.; Xu, L. Change of indocyanine green clearance ability and liver function after transcatheter intra-arterial therapies and its impact on outcomes of resectable hepatocellular carcinoma: a retrospective cohort study. *Int J Surg* 2024, *110*, 2832-2844, https://doi.org/10.1097/JS9.0000000000001156

[17] Ishizawa, T.; Fukushima, N.; Shibahara, J.; Masuda, K.; Tamura, S.; Aoki, T.; Hasegawa, K.; Beck, Y.; Fukayama, M.; Kokudo, N. Real-time identification of liver cancers by using indocyanine green fluorescent imaging. *Cancer* 2009, *115*, 2491-2504, https://doi.org/10.1002/cncr.24291

[18] Takemura, N.; Ito, K.; Inagaki, F.; Mihara, F.; Kokudo, N. Added value of indocyanine green fluorescence imaging in liver surgery. *Hepatobiliary Pancreat Dis Int* 2021, *21*, 310-317, https://doi.org/10.1016/j.hbpd.2021.12.007

[19] Sangro, B.; Sarobe, P.; Hervás-Stubbs, S.; Melero, I. Advances in immunotherapy for hepatocellular carcinoma. *Nat Rev Gastroenterol Hepatol* 2021, *18*, 525-543, https://doi.org/10.1038/s41575-021-00438-0

[20] Wang, X.; Teh, C. S. C.; Ishizawa, T.; Aoki, T.; Cavallucci, D.; Lee, S.-Y.; Panganiban, K. M.; Perini, M. V.; Shah, S. R.; Wang, H.; et al. Consensus Guidelines for the Use of Fluorescence Imaging in Hepatobiliary Surgery. *Ann Surg* 2021, *274*, https://doi.org/10.1097/SLA.0000000000004718

[21] Marubashi, S.; Gotoh, K.; Akita, H.; Takahashi, H.; Ito, Y.; Yano, M.; Ishikawa, O.; Sakon, M. Anatomical versus non-anatomical resection for hepatocellular carcinoma. *Br J Surg* 2015, *102*, 776-784, https://doi.org/10.1002/bjs.9815

[22] Liu, J.; Zhuang, G.; Bai, S.; Hu, Z.; Xia, Y.; Lu, C.; Wang, J.; Wang, C.; Liu, L.; Li, F.; et al. The Comparison of Surgical Margins and Type of Hepatic Resection for Hepatocellular Carcinoma With Microvascular Invasion. *Oncologist* 2023, *28*, e1043-e1051, https://doi.org/10.1093/oncolo/oyad124

Research Field

Man Luo: Liver Tumor, Hepatobiliary Surgery, Hepatocellular carcinoma, cholangiocarcinoma

Yue Liu: Liver Tumor, Hepatobiliary Surgery

Yaowei Hu: Liver Tumor, Hepatobiliary Surgery

Hongguang Wang: Liver Tumor, Hepatobiliary Surgery, Hepatocellular carcinoma, cholangiocarcinoma, Intrahepatic ultrasound